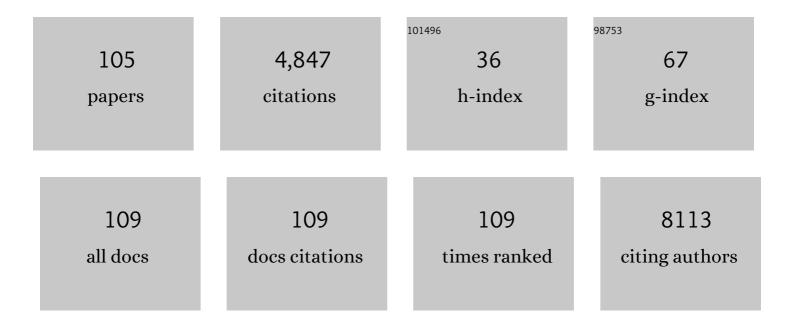
List of Publications by Year in descending order

Source: https://exaly.com/author-pdf/8350432/publications.pdf Version: 2024-02-01



#	Article	IF	CITATIONS
1	Gut Microbiota Orchestrates Energy Homeostasis during Cold. Cell, 2015, 163, 1360-1374.	13.5	581
2	Multivalent Effects of RGD Peptides Obtained by Nanoparticle Display. Journal of Medicinal Chemistry, 2006, 49, 6087-6093.	2.9	355
3	Microbiota depletion promotes browning of white adipose tissue and reduces obesity. Nature Medicine, 2015, 21, 1497-1501.	15.2	324
4	Nanoparticle Imaging of Integrins on Tumor Cells. Neoplasia, 2006, 8, 214-222.	2.3	226
5	Computed tomography of the chest with model-based iterative reconstruction using a radiation exposure similar to chest X-ray examination: preliminary observations. European Radiology, 2013, 23, 360-366.	2.3	188
6	Tomographic Fluorescence Mapping of Tumor Targets. Cancer Research, 2005, 65, 6330-6336.	0.4	176
7	Interaction of Functionalized Superparamagnetic Iron Oxide Nanoparticles with Brain Structures. Journal of Pharmacology and Experimental Therapeutics, 2006, 318, 108-116.	1.3	168
8	Imaging Pancreatic Cancer with a Peptideâ^'Nanoparticle Conjugate Targeted to Normal Pancreas. Bioconjugate Chemistry, 2006, 17, 905-911.	1.8	145
9	Targeting Vascular NADPH Oxidase 1 Blocks Tumor Angiogenesis through a PPARα Mediated Mechanism. PLoS ONE, 2011, 6, e14665.	1.1	128
10	Tomographic Fluorescence Imaging of Tumor Vascular Volume in Mice. Radiology, 2007, 242, 751-758.	3.6	115
11	Insertion of Nanoparticle Clusters into Vesicle Bilayers. ACS Nano, 2014, 8, 3451-3460.	7.3	82
12	Surgical management of adrenal metastases. Langenbeck's Archives of Surgery, 2012, 397, 179-194.	0.8	76
13	Nanoparticles for the Optical Imaging of Tumor selectin. Neoplasia, 2005, 7, 904-911.	2.3	69
14	Adapting anatomy teaching to surgical trends: a combination of classical dissection, medical imaging, and 3D-printing technologies. Surgical and Radiologic Anatomy, 2016, 38, 361-367.	0.6	67
15	Ultrasound diagnosis of anterior iliopsoas impingement in total hip replacement. Skeletal Radiology, 2004, 33, 112-116.	1.2	65
16	Clot-Based Radiomics Predict a Mechanical Thrombectomy Strategy for Successful Recanalization in Acute Ischemic Stroke. Stroke, 2020, 51, 2488-2494.	1.0	63
17	Incidental adrenal lesions detected on enhanced abdominal dual-energy CT: Can the diagnostic workup be shortened by the implementation of virtual unenhanced images?. European Journal of Radiology, 2014, 83, 1746-1751.	1.2	57
18	Low-dose computed tomography for the diagnosis of pneumonia in elderly patients: a prospective, interventional cohort study. European Respiratory Journal, 2018, 51, 1702375.	3.1	56

#	Article	IF	CITATIONS
19	Simultaneous fluorescence imaging of protease expression andÂvascularity during murine colonoscopy for colonic lesion characterization. Gastrointestinal Endoscopy, 2006, 64, 589-597.	0.5	52
20	Inflow effect correction in fast gradient-echo perfusion imaging. Magnetic Resonance in Medicine, 2003, 50, 885-891.	1.9	51
21	Hepatic PTEN deficiency improves muscle insulin sensitivity and decreases adiposity in mice. Journal of Hepatology, 2015, 62, 421-429.	1.8	49
22	Participation in lung cancer screening programs: are there gender and social differences? A systematic review. Public Health Reviews, 2018, 39, 23.	1.3	49
23	Ectopic UCP1 Overexpression in White Adipose Tissue Improves Insulin Sensitivity in Lou/C Rats, a Model of Obesity Resistance. Diabetes, 2015, 64, 3700-3712.	0.3	48
24	What is the diagnostic performance of 18-FDG-PET/MR compared to PET/CT for the N- and M- staging of breast cancer?. European Radiology, 2019, 29, 1787-1798.	2.3	48
25	Magnetic Resonance Imaging With Hepatospecific Contrast Agents in Cirrhotic Rat Livers. Investigative Radiology, 2005, 40, 187-194.	3.5	47
26	Diagnostic accuracy of digitized periapical radiographs validated against micro omputed tomography scanning in evaluating orthodontically induced apical root resorption. European Journal of Oral Sciences, 2008, 116, 467-472.	0.7	47
27	Differentiating kidney stones from phleboliths in unenhanced low-dose computed tomography using radiomics and machine learning. European Radiology, 2019, 29, 4776-4782.	2.3	47
28	Noninvasive Measurement of Absolute Renal Perfusion by Contrast Medium-Enhanced Magnetic Resonance Imaging. Investigative Radiology, 2003, 38, 584-592.	3.5	46
29	Kinetics of Gadobenate Dimeglumine in Isolated Perfused Rat Liver: MR Imaging Evaluation. Radiology, 2003, 229, 119-125.	3.6	45
30	Clinical utility of 18F-FDG-PET/MR for preoperative breast cancer staging. European Radiology, 2016, 26, 2297-2307.	2.3	45
31	Model-Based Iterative Reconstruction (MBIR) for the Reduction of Metal Artifacts on CT. American Journal of Roentgenology, 2015, 205, 380-385.	1.0	44
32	Cell Internalization of Magnetic Nanoparticles Using Transfection Agents. Molecular Imaging, 2007, 6, 7290.2006.00028.	0.7	43
33	Molecular imaging by micro-CT: specific E-selectin imaging. European Radiology, 2009, 19, 2487-2494.	2.3	42
34	Improved Visualization of Vessels and Hepatic Tumors by Micro-Computed Tomography (CT) Using Iodinated Liposomes. Investigative Radiology, 2007, 42, 652-658.	3.5	41
35	High-resolution sonography of compressive neuropathies of the wrist. Journal of Clinical Ultrasound, 2004, 32, 451-461.	0.4	40
36	High-Resolution Magnetic Resonance Imaging Quantitatively Detects Individual Pancreatic Islets. Diabetes, 2011, 60, 2853-2860.	0.3	38

XAVIER MONTET

#	Article	IF	CITATIONS
37	Radiomics and Machine Learning Differentiate Soft-Tissue Lipoma and Liposarcoma Better than Musculoskeletal Radiologists. Sarcoma, 2020, 2020, 1-9.	0.7	38
38	Transfection Agent Induced Nanoparticle Cell Loading. Molecular Imaging, 2005, 4, 153535002005051.	0.7	37
39	In vivo labelling of resting monocytes in the reticuloendothelial system with fluorescent iron oxide nanoparticles prior to injury reveals that they are mobilized to infarcted myocardium. European Heart Journal, 2010, 31, 1410-1420.	1.0	37
40	Accuracy of cone-beam computed tomography for syndesmosis injury diagnosis compared to conventional computed tomography. Foot and Ankle Surgery, 2020, 26, 265-272.	0.8	36
41	Superparamagnetic nanoparticles - a tool for early diagnostics. Swiss Medical Weekly, 2010, 140, w13081.	0.8	36
42	The Empty Azygos Fissure. Journal of Radiology Case Reports, 2013, 7, 10-5.	0.2	34
43	Respiratory-Gated MRgHIFU in Upper Abdomen Using an MR-Compatible In-Bore Digital Camera. BioMed Research International, 2014, 2014, 1-9.	0.9	33
44	Imaging of fractures of the lateral process of the talus, a frequently missed diagnosis. European Journal of Radiology, 2003, 47, 64-70.	1.2	32
45	Macrophage migration inhibitory factor deficiency leads to age-dependent impairment of glucose homeostasis in mice. Journal of Endocrinology, 2010, 206, 297-306.	1.2	30
46	The Lou/C rat: a model of spontaneous food restriction associated with improved insulin sensitivity and decreased lipid storage in adipose tissue. American Journal of Physiology - Endocrinology and Metabolism, 2009, 296, E1120-E1132.	1.8	29
47	Experimental noninferiority trial of synthetic small-caliber biodegradable versus stable vascular grafts. Journal of Thoracic and Cardiovascular Surgery, 2013, 146, 400-407.e1.	0.4	28
48	DIEP flap for breast reconstruction: IsÂabdominal fat thickness associated with post-operative complications?. Journal of Plastic, Reconstructive and Aesthetic Surgery, 2017, 70, 1068-1075.	0.5	28
49	Magnetic Resonance–Guided Shielding of Prefocal Acoustic Obstacles in Focused Ultrasound Therapy. Investigative Radiology, 2013, 48, 366-380.	3.5	27
50	Urinary stone detection and characterisation with dual-energy CT urography after furosemide intravenous injection: preliminary results. European Radiology, 2014, 24, 709-714.	2.3	27
51	Hyaluronic Acid Filler in HIV-Associated Facial Lipoatrophy: Evaluation of Tissue Distribution and Morphology with MRI. Dermatology, 2015, 230, 367-374.	0.9	27
52	Intramuscular ganglion arising from the acromioclavicular joint. Clinical Imaging, 2004, 28, 109-112.	0.8	25
53	Pancreatic magnetic resonance imaging after manganese injection distinguishes type 2 diabetic and normoglycemic patients. Islets, 2012, 4, 243-248.	0.9	24
54	Targeting GLP-1 receptors for repeated magnetic resonance imaging differentiates graded losses of pancreatic beta cells in mice. Diabetologia, 2015, 58, 304-312.	2.9	24

#	Article	IF	CITATIONS
55	Radiological findings of complications after lung transplantation. Insights Into Imaging, 2018, 9, 709-719.	1.6	24
56	Sonographic and MRI appearance of tensor fasciae suralis muscle, an uncommon cause of popliteal swelling. Skeletal Radiology, 2002, 31, 536-538.	1.2	23
57	Female Hydrocele: The Cyst of Nuck. Urologia Internationalis, 2009, 82, 242-245.	0.6	22
58	Genetic Ablation of MiR-22 Fosters Diet-Induced Obesity and NAFLD Development. Journal of Personalized Medicine, 2020, 10, 170.	1.1	21
59	Orthodontically induced cervical root resorption in humans is associated with the amount of tooth movement. European Journal of Orthodontics, 2017, 39, 534-540.	1.1	20
60	Mild hyperthermia by MR-guided focused ultrasound in an ex vivo model of osteolytic bone tumour: optimization of the spatio-temporal control of the delivered temperature. Journal of Translational Medicine, 2019, 17, 350.	1.8	20
61	Treatment with direct-acting antivirals improves peripheral insulin sensitivity in non-diabetic, lean chronic hepatitis C patients. PLoS ONE, 2019, 14, e0217751.	1.1	20
62	Enzyme-based visualization of receptor–ligand binding in tissues. Laboratory Investigation, 2006, 86, 517-525.	1.7	18
63	Model-Based Iterative Reconstruction Versus Adaptive Statistical Iterative Reconstruction in Low-Dose Abdominal CT for Urolithiasis. American Journal of Roentgenology, 2014, 203, 336-340.	1.0	18
64	Rational Use of CT-Scan for the Diagnosis of Pneumonia: Comparative Accuracy of Different Strategies. Journal of Clinical Medicine, 2019, 8, 514.	1.0	17
65	Mir-21 Suppression Promotes Mouse Hepatocarcinogenesis. Cancers, 2021, 13, 4983.	1.7	17
66	Generative Adversarial Networks Improve the Reproducibility and Discriminative Power of Radiomic Features. Radiology: Artificial Intelligence, 2020, 2, e190035.	3.0	16
67	Image quality of low mA CT pulmonary angiography reconstructed with model based iterative reconstruction versus standard CT pulmonary angiography reconstructed with filtered back projection: an equivalency trial. European Radiology, 2015, 25, 1665-1671.	2.3	15
68	Diagnosis of Urothelial Tumors With a Dedicated Dual-Source Dual-Energy MDCT Protocol: Preliminary Results. American Journal of Roentgenology, 2014, 202, W357-W364.	1.0	14
69	Periodontal parameters and cervical root resorption during orthodontic tooth movement. Journal of Clinical Periodontology, 2008, 35, 501-506.	2.3	13
70	Alterations in lipid metabolism and thermogenesis with emergence of brown adipocytes in white adipose tissue in diet-induced obesity-resistant Lou/C rats. American Journal of Physiology - Endocrinology and Metabolism, 2011, 300, E1146-E1157.	1.8	13
71	Impact of iterative reconstructions on objective and subjective emphysema assessment with computed tomography: a prospective study. European Radiology, 2017, 27, 2950-2956.	2.3	13
72	Supraposition of unopposed molars in young and adult rats. Archives of Oral Biology, 2009, 54, 40-44.	0.8	12

#	Article	IF	CITATIONS
73	Fat suppression techniques for breast MRI: Dixon versus spectral fat saturation for 3D T1-weighted at 3ÂT. Radiologia Medica, 2017, 122, 731-742.	4.7	12
74	Evaluating the effect of increased pitch, iterative reconstruction and dual source CT on dose reduction and image quality. British Journal of Radiology, 2018, 91, 20170443.	1.0	12
75	Metallic artifact reduction by evaluation of the additional value of iterative reconstruction algorithms in hip prosthesis computed tomography imaging. Medicine (United States), 2019, 98, e14341.	0.4	12
76	ECG-triggered high-pitch CT for simultaneous assessment of the aorta and coronary arteries. Journal of Cardiovascular Computed Tomography, 2016, 10, 407-413.	0.7	10
77	Assessment of intra-articular volume of the wrist: a comparative study between CT-arthrography and dissection. Surgical and Radiologic Anatomy, 2005, 27, 444-449.	0.6	9
78	Multivalent glibenclamide to generate islet specific imaging probes. Biomaterials, 2016, 75, 1-12.	5.7	9
79	Dual-energy computed tomographic imaging of pulmonary hypertension. Swiss Medical Weekly, 2016, 146, w14328.	0.8	9
80	An Albumin-Activated Far-Red Fluorochrome for Inâ€Vivo Imaging. ChemMedChem, 2006, 1, 66-69.	1.6	8
81	Échographie desÂnerfs desÂmembres inférieurs. Revue Du Rhumatisme (Edition Francaise), 2007, 74, 415-423.	0.0	7
82	A New MDCT Technique for the Detection and Anatomical Exploration of Urogenital Fistulas. American Journal of Roentgenology, 2012, 198, W160-W162.	1.0	7
83	Standardized fluoroscopyâ€based technique to measure intraoperative cup anteversion. Journal of Orthopaedic Research, 2017, 35, 2307-2312.	1.2	7
84	Low lodine Contrast Injection for CT Acquisition Prior to Transcatheter Aortic Valve Replacement: Aorta Assessment and Screening for Coronary Artery Disease. Academic Radiology, 2019, 26, e150-e160.	1.3	7
85	Value of liver computed tomography with iodixanol 270, 80 kVp and iterative reconstruction. World Journal of Radiology, 2016, 8, 693.	0.5	7
86	Long-Term Survival with Regorafenib in KRAS-Mutated Metastatic Rectal Cancer. Case Reports in Oncology, 2018, 10, 1029-1034.	0.3	6
87	Wet avalanches: long-term evolution in the Western Alps under climate and human forcing. Climate of the Past, 2018, 14, 1299-1313.	1.3	6
88	Iterative Algorithms Applied to Treated Intracranial Aneurysms. Clinical Neuroradiology, 2019, 29, 741-749.	1.0	6
89	Pulmonary Perfusion Changes as Assessed by Contrast-Enhanced Dual-Energy Computed Tomography after Endoscopic Lung Volume Reduction by Coils. Respiration, 2016, 92, 404-413.	1.2	5
90	CT vaginography: a new CT technique for imaging of upper and middle vaginal fistulas. British Journal of Radiology, 2017, 90, 20160947.	1.0	5

#	Article	IF	CITATIONS
91	Prostatic Utricle Cyst as the Most Likely Cause in a Case of Recurrent Episodes of Hematospermia. Case Reports in Urology, 2017, 2017, 1-3.	0.1	5
92	lmaging patterns of Pneumocystis jirovecii pneumonia in HIV-positive and renal transplant patients – a multicentre study. Swiss Medical Weekly, 2019, 149, w20130.	0.8	5
93	Ossifying metaplasia of urothelial metastases: original case with review of the literature. BMC Medical Imaging, 2015, 15, 30.	1.4	4
94	Emphysema quantification using hybrid versus model-based generations of iterative reconstruction. Medicine (United States), 2019, 98, e14450.	0.4	4
95	Gastrointestinal relapse of multiple myeloma and sustained response to lenalidomide: a case report. Journal of Medical Case Reports, 2011, 5, 110.	0.4	3
96	Classification of magnetic resonance images from rabbit renal perfusion. Chemometrics and Intelligent Laboratory Systems, 2009, 98, 173-181.	1.8	2
97	Colovesical fistula causing an uncommon reason for failure of computed tomography colonography: a case report. Journal of Medical Case Reports, 2012, 6, 214.	0.4	2
98	Ampullary micropapillary adenocarcinoma widely metastatic to the lymph nodes: A case report. Human Pathology: Case Reports, 2018, 14, 12-15.	0.2	2
99	Clitoral Anatomy, Physiology and Pathology Demystified by Imaging. Current Medical Imaging, 2018, 14, 366-373.	0.4	1
100	About a case of pulmonary blastoma. European Journal of Radiology Extra, 2004, 49, 17-21.	0.1	0
101	Tumor Imaging. , 0, , 277-309.		0
102	Approaches for Imaging Pancreatic Islets: Recent Advances and Future Prospects. , 2015, , 59-81.		0
103	Scintigraphic Identification of Gastric Tissue in a Mediastinal Mass. Clinical Nuclear Medicine, 2016, 41, 207-208.	0.7	Ο
104	MAGNETIC RESONANCE AND BIOLUMINESCENCE IMAGING MONITOR QUANTITATIVE DIFFERENCES IN PANCREATIC ISLETS AND THEIR REGENERATION AFTER BETA CELL LOSS. FASEB Journal, 2013, 27, 531.2.	0.2	0
105	Approaches for Imaging Pancreatic Islets: Recent Advances and Future Prospects. , 2014, , 1-21.		Ο